Polish J. Chem., **75**, 463–479 (2001) **REVIEW ARTICLE**

Anchoring, Wetting and Symmetry-Breaking Surface Transition in Liquid Crystal Systems*

by A. Poniewierski and A. Samborski

Institute of Physical Chemistry, Polish Academy of Sciences, Kasprzaka 44/52, 01-224 Warsaw, Poland

(Received October 26th, 2000)

A nematic liquid crystal in contact with a solid substrate is considered. Three types of surface phenomena are discussed: anchoring, wetting and surface phase transitions, which involve symmetry breaking in the surface layer. Where possible, we reveal relations between these phenomena. We concentrate on the following problems: anchoring on anisotropic substrates, the force balance equation at the nematic-isotropic-substrate contact line, the behaviour of the line tension in the thermodynamic limit, and the onset of the smectic-A order in the surface layer close to the bulk transition to the smectic-A phase. All these problems are studied in the framework of the Landau-de Gennes formalism. Possible directions of future studies are discussed.

Key words: phase transitions, liquid crystals, surface phenomena, anchoring, wetting

I. INTRODUCTION

In liquid crystals the molecular orientational degrees of freedom have a great influence on the fluid structure [1]. The presence of orientational order is a characteristic feature of all liquid crystal phases. While in the nematic phase this is the only type of order, smectic phases have in addition a layered structure. Thus, they also exhibit a positional order at least in one dimension. The direction of preferred molecular alignment, defined by a unit vector $\hat{\mathbf{n}}$ called the director, can be manipulated with electric and magnetic fields, and also through coupling to surfaces. Needless to say, the practical applications of liquid crystals in electro-optical devices are based on this phenomenon.

In the absence of bulk external fields, a particular orientation of $\hat{\mathbf{n}}$ in a liquid crystal sample can be achieved due to a limiting surface, *e.g.*, the surface of a substrate in contact with the liquid crystal. The effect of the surface on orientation of $\hat{\mathbf{n}}$ is twofold. Firstly, it breaks the translational symmetry of the sample. Thus, a molecule close to the surface has fewer nearest neighbours than a molecule in the bulk, which effectively modifies the fluid-fluid interactions in the layer adjacent to the substrate. Secondly, the direct fluid-substrate interactions may favour a particular orientation of

* Dedicated to Prof. Jan Stecki on the occasion of his 70th birthday.

molecules with respect to the surface. In consequence, there exists a set of orientations of $\hat{\mathbf{n}}$, discrete or continuous, for which the free energy of the liquid crystal is minimal. This phenomenon is called anchoring [2,3], and the anchoring direction corresponds to the minimum of the free energy. The orientation of $\hat{\mathbf{n}}$, chosen by the surface, depends on the details of both the fluid-fluid and the fluid-substrate interactions. Moreover, the symmetry of the substrate is also an important factor [4–17]. Therefore, various types of anchoring can be observed. For isotropic substrates, anchoring can be either monostable or continuously degenerated. In the first case $\hat{\mathbf{n}}$ is perpendicular to the surface (homeotropic anchoring), whereas in the second case $\hat{\mathbf{n}}$ is either in the plane of the surface (planar anchoring) or tilted with respect to it (conical anchoring). A discrete set of anchoring directions can be obtained in the case of anisotropic substrates. Examples of anisotropic substrates are SiO_x films evaporated under oblique incidence [4–6] or microtextured substrates [18,19].

When a liquid crystal phase coexists with an isotropic phase, which can be either an isotropic liquid or a vapour, or when two liquid crystal phases coexist, then the interface between two phases plays the role of a limiting surface. The presence of the interface breaks the translational symmetry of the system. Since spatial inhomogeneities couple to orientational degrees of freedom, the orientational symmetry is also broken. In other words, there exist orientations of $\hat{\mathbf{n}}$ preferred by the interface, and this phenomenon is known as anchoring at the interface. It is analogous to anchoring on a solid substrate, although it occurs entirely due to modification of the effective fluid-fluid interactions in the inhomogeneous interfacial region. The simplest examples of liquid crystal interfaces are the nematic-isotropic (NI) and the nematic-vapour (NV) interfaces.

In the absence of bulk external fields, anchoring is responsible for the average orientation of liquid crystal molecules in the bulk. However, anchoring is a surface phenomenon, as it stems from the presence of a limiting surface in the system. While orientational anchoring is specific to liquid crystal systems, wetting – another well known surface phenomenon – can be observed in very different systems such as simple and complex fluids, mixtures, and solids [20–23]. Wetting may occur whenever two phases coexist in the presence of a third spectator phase. Here, we restrict ourselves to two-fluid phase coexistence when the spectator phase is a rigid solid. Then the balance of forces at the contact line leads to the Young condition, which relates the contact angle with the three surface tensions. If the contact angle is different from zero or π, partial wetting occurs. Otherwise wetting is complete, which means that a macroscopic film of one of the coexisting phases completely covers the spectator phase. Compared to simple fluids and their mixtures, wetting in liquid crystal systems is much more complex, since it involves not only variations of the density or concentrations but also variations of the local symmetry axes and order parameters. Recently, there has been a growing interest in the relation between wetting and anchoring in liquid crystal systems [24–28]. In the context of partial wetting, it is natural to ask whether the Young condition is modified, if there is a liquid-crystalline phase involved, and if it is, how it is related to anchoring.

A third kind of surface phenomena, which have no counterpart in simple fluid systems, is surface symmetry-breaking transition. For instance, let us consider a liquid crystalline phase in contact with a solid substrate. It is possible that when the transition to another liquid-crystalline phase of lower symmetry is approached, the onset of the new phase first appears in a thin surface layer, while the bulk remains in the higher symmetry state. An example of such a transition is the onset of the nematic phase in the surface layer when the bulk fluid is still isotropic [29–31]. It can occur when the planar alignment of molecules at the substrate is preferred. Then the uniaxial symmetry of the system can be broken and a biaxial surface layer appears. This uniaxial-biaxial surface transition was predicted some time ago in the framework of a Landau-de Gennes model. Later theoretical studies and very recent computer simulations of hard rods at a hard wall have confirmed these predictions [32,33].

Above we have outlined three kinds of surface phenomena in liquid crystal systems. The purpose of this short review is to present specific examples of these surface phenomena and, where possible, to show relations between them. The plan of the paper is as follows: In the next section we consider anchoring on anisotropic substrates. In section III, we derive a generalized Young equation for the nematic-isotropic-substrate contact line in conditions of partial wetting of the substrate by the nematic phase. Section IV is devoted to a surface phase transition, in which a smectic-A surface order appears above the bulk nematic–smectic-A transition. All these problems are studied in the framework of the Landau-de Gennes formalism. Finally, the conclusions and discussion are presented in section V.

II. ANCHORING ON ANISOTROPIC SUBSTRATES

Let us consider a nematic liquid crystal in contact with a flat solid substrate. The z axis of the coordiante system is oriented normal to the surface of the substrate, which is at $z = 0$. The limit $z \to \infty$ corresponds to the bulk nematic phase. To describe the system on a mesoscopic scale we use the Landau-de Gennes theory of non-uniform nematic liquid crystals [1,23,34,35]. We neglect the density changes and assume that the only relevant variable is the nematic order parameter $\mathbf{Q}$, a second rank, traceless and symmetric tensor. In general, $\mathbf{Q}$ has five independent components but this number can be reduced if there are some symmetries in the sytem.

The free energy density, f, has two contributions: the Landau free energy of a uniform system, f_L, which must describe the NI coexistence, and the contribution due to non-uniformities, f_G, which has a square-gradient form. Thus, we have

$$f = f_L + f_G \tag{2.1a}$$

$$f_L = ATr\mathbf{Q}^2 - BTr\mathbf{Q}^3 + C(Tr\mathbf{Q}^2)^2 \tag{2.1b}$$

$$f_G = 1/2(L_1\partial_k Q_{ij}\partial_k Q_{ij} + L_2\partial_j Q_{ij}\partial_k Q_{ik} + L_3\partial_k Q_{ij}\partial_j Q_{ik}) \tag{2.1c}$$

where the indices run over x, y, z, $\partial_k = \partial/\partial r_k$, and the summation convention is assumed. A is proportional to the temperature difference $T - T^*$, where T^* denotes the limit of stability of the isotropic phase, and B and C, together with the elastic constants L_1, L_2 and L_3, are temperature independent material constants.

The interaction of the liquid crystal with the solid substrate is mimicked by a surface free energy density, $f_s(\mathbf{Q}_0)$, where $\mathbf{Q}_0 = \mathbf{Q}(x, y, z = 0)$. The excess free energy due to the presence of the substrate is a functional of $\mathbf{Q}$ given by

$$F[\mathbf{Q}] = \int d^3r[f(\mathbf{Q}, \nabla\mathbf{Q}) - f_b + \delta(z) f_s(\mathbf{Q})] \tag{2.2}$$

where f_b is the free energy density in the bulk, and $\delta(z)$ is the one-dimensional Dirac delta function. This is the general form of the free energy functional. In this section, however, we assume that $\mathbf{Q}$ depends only on z. Thus, the integration over the plane parallel to the substrate (the xy plane) can be performed. To reduce the number of independent phenomenological parameters we assume f_s in the following simple form [36]

$$f_s = -Tr(\mathbf{h}\cdot\mathbf{Q}) \tag{2.3}$$

where the surface field $\mathbf{h}$ can also be chosen as a symmetric and traceless tensor. The molecular origin of (2.3) is the direct interaction between the liquid crystal molecules and the substrate. A more general form of f_s should also contain quadratic terms, which correspond to the modification of the fluid-fluid interactions in the surface layer. However, to study the effect of the reduced symmetry of the substrate on anchoring directions it is sufficient to consider only linear terms.

The form of f_s must be compatible with the symmetry of the substrate. In the isotropic case, the only non-vanishing components of $\mathbf{h}$ are: $h_{xx} = h_{yy} = -1/2h_{zz}$, hence, $f_s = -3/2h_{zz}Q_{zz}$. Depending on the sign of h_{zz} this leads to either homeotropic or planar anchoring. A more interesting situation occurs when the substrate is anisotropic. In other words, a particular direction in the xy plane has been chosen by some physical process, and we assume that it is along the x axis. Moreover, we assume that the substrate has the mirror symmetry $y \to -y$. Then $h_{xy} = h_{yz} = 0$, thus, $\mathbf{h}$ has three independent components: h_{xz} and two diagonal components. The latter can be chosen at convenience but have to satisfy the condition $Tr\mathbf{h} = 0$.

To obtain the anchoring directions we follow the standard procedure of minimization of the free energy functional. This leads to a set of Euler-Lagrange equations which have to be solved with proper boundary conditions. The details are presented in [36], and here we only summarize the main results. In Fig. 1, we present schematically all anchoring directions compatible with the symmetry of the substrate assumed above. There are four possible states. Two of them correspond to the bulk director in the xz plane, which is the mirror symmetry plane. These two states are referred to as

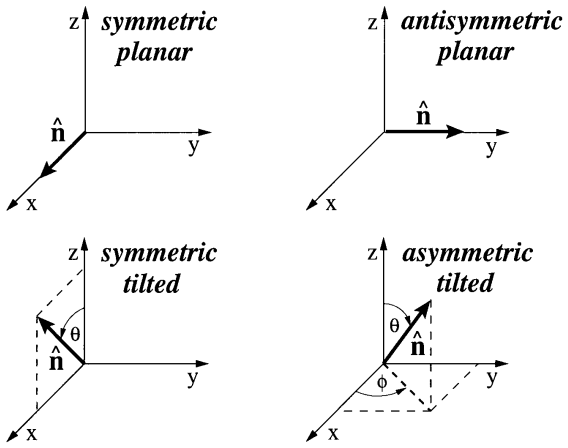

Figure 1. Schematic picture of all types of anchoring discussed in the text. The *xz* plane is the mirror symmetry plane. θ and ϕ are the polar and the azimuthal angles, respectively. In the antisymmetric planar case, the orientations $\hat{\mathbf{n}}$ and $-\hat{\mathbf{n}}$ are equivalent. In the asymmetric tilted case, $\hat{\mathbf{n}}$ and its mirror image with respect to the *xz* plane correspond to the same free energy.

symmetric anchoring. When $\hat{\mathbf{n}}$ is parallel to the *x* axis we call it symmetric planar anchoring, otherwise, it is called symmetric tilted anchoring. In both cases anchoring is monostable, as the directions *x* and *–x* are not equivalent. The remaining two states correspond, respectively, to the antisymmetric planar anchoring, with $\hat{\mathbf{n}}$ along the *y* axis, and the asymmetric tilted anchoring, with $\hat{\mathbf{n}}$ tilted with respect to all three axes. Since $\hat{\mathbf{n}}$ and its mirror image with respect to the *xz* plane correspond to the same free energy asymmetric tilted anchoring is bistable. Note that antisymmetric planar anchoring is monostable as the orientations $\hat{\mathbf{n}}$ and $-\hat{\mathbf{n}}$ are physically equivalent.

To present the phase diagram at constant temperature we express the tensor **h** as follows: $\mathbf{h} = h_1(1/3\mathbf{I} - \hat{\mathbf{y}}\hat{\mathbf{y}}) + h_2(\hat{\mathbf{z}}\hat{\mathbf{z}} - \hat{\mathbf{x}}\hat{\mathbf{x}}) + h_3(\hat{\mathbf{x}}\hat{\mathbf{z}} + \hat{\mathbf{z}}\hat{\mathbf{x}})$, where **I** is the unit tensor. Here we choose the plane $h_2 = -h_1$, for which $f_s = -2h_1Q_{xx} - 2h_3Q_{xz}$. The phase diagram corresponding to this particular choice of surface fields and to the temperature $T = T^*$ is shown in Fig. 2. For $h_1 > 0$ and $h_3 \neq 0$, f_s favours $Q_{xx} > 0$ and $Q_{xz} \neq 0$. Thus, the only stable phase in this region is the symmetric tilted phase. For h_1 less than some $h_{1c} < 0$, there is a region of stability of the asymmetric tilted phases. In this region, none of the off-diagonal components of **Q** vanish. For $h_{1c} < h_1 < 0$ and h_3 around zero, the antisymmetric planar phase is stable. These two regions are separated by a line of critical points, at which the difference between the asymmetric tilted phases disappears, *i.e.*, Q_{xy} and Q_{yz} vanish. Q_{xy} and Q_{yz} also vanish at the asymmetric tilted-symmetric tilted transition, which is also continuous.

Since the phase diagram is presented in the space of surface fields, for a fixed temperature, different values of these fields correspond to different substrates. This resembles the experimental situation with SiO_x films evaporated under oblique incidence, where different types of anchoring are obtained by changing the incidence

angle. Comparison of the experimental results with the predictions of the Landau-de Gennes model shows that an increase of the incidence angle has the same effect as an increase of the *xz* component of **h**.

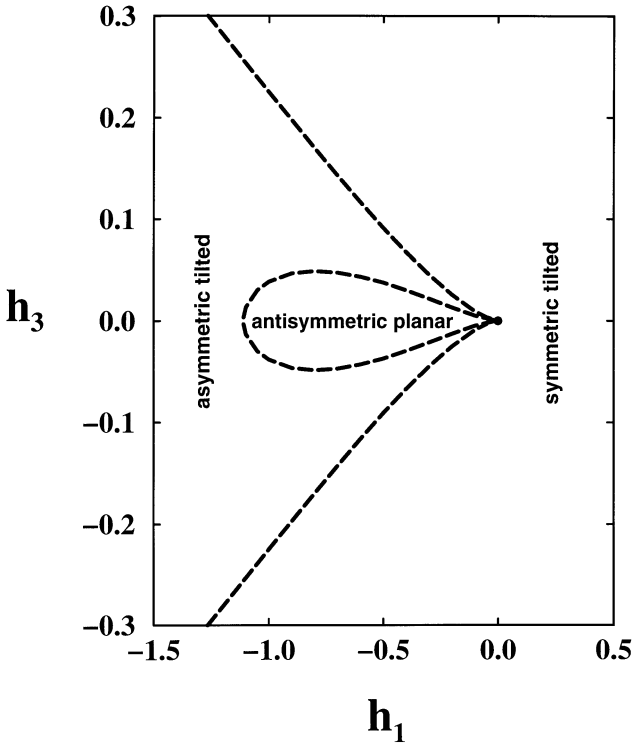

Figure 2. Phase diagram in the (h_1, h_3) plane, for $h_2 = -h_1$ and $T = T^*$. The dashed lines show the continuous transitions. In the asymmetric tilted region, two asymmetric tilted phases coexist. The difference between these two phases disappears along the lines of continuous transitions to the antisymmetric planar phase or the symmetric tilted phase.

III. A GENERALIZED YOUNG CONDITION AT THE NEMATIC-ISOTROPIC-SUBSTRATE CONTACT LINE

When two fluid phases coexist in presence of a solid substrate one can observe a three-phase contact line [20,37]. In equilibrium, the contact line must be at rest, and the balance of forces due to the three surface tensions leads to the famous Young condition. In the case of the nematic-isotropic-substrate contact line

$$\gamma_{IS} = \gamma_{NS} + \gamma_{NI}\cos\alpha_c \tag{3.1}$$

where γ_{IS}, γ_{NS} and γ_{NI} denote the surface tensions of the isotropic-substrate, the nematic-substrate and the nematic-isotropic interfaces, respectively. α_c is the contact

angle at which the NI interface is tilted with respect to the substrate at the contact line. If $0 < \alpha_c < \pi/2$ wetting of the substrate by the nematic phase is partial. The contact angle is a macroscopic concept. In general, there exists a core region in the vicinity of the contact line, in which the tilt angle of the fluid-fluid interface can differ from α_c. However, a well defined contact angle is measured provided the distance from the contact line is large compared to the size of the core region but small compared to the radii of curvature of the droplet. The excess free energy of the inhomogeneous region around the contact line is known as the line tension [37]. The line tension in simple fluid systems, in particular, its behaviour close to the transition from partial to complete wetting, has been studied by several authors [38–42].

In model studies of the inhomogeneous contact line region, it is convenient to neglect all curvature effects and consider the geometry of a liquid wedge rather than a drop. Thus, the system is homogeneous along the contact line, which is now a straight line. We choose the *y* axis to be oriented parallel to the contact line. In the remaining two directions the system is inhomgeneous. The distance from the contact line is measured along the *x* direction, while the *z* direction is normal to the substrate. Here, we consider three possible configurations of the director field when anchoring at the NS and the NI interfaces is either planar or homeotropic (see Fig. 3). In all cases presented in Fig. 3, $\hat{\mathbf{n}}$ is in the plane of the figure (the *xz* plane). Note that if anchoring at both interfaces was planar then the orientation of $\hat{\mathbf{n}}$ parallel to the contact line would be energetically favourable.

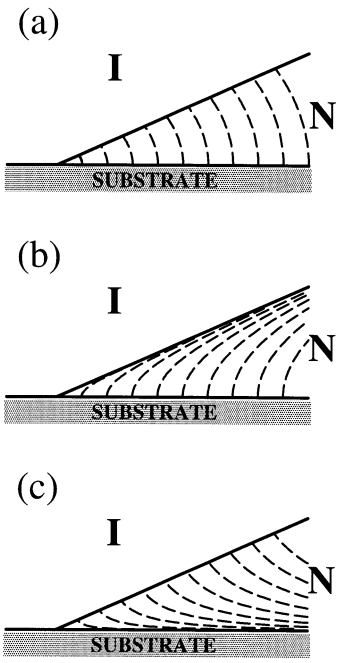

Figure 3. Schematic picture of the asymptotic director field for the liquid wedge geometry. Anchoring at the NS and the NI interfaces is, respectively, (a) homeotropic and homeotropic, (b) homeotropic and planar, (c) planar and homeotropic.

An elastic deformation of the director field decays inversely proportional with the distance between the interfaces and, in consequence, also with the distance from the contact line. Because of this slow decay, the following interesting questions arise. (1) Is the Young condition modified due to the deformation of the director field? (2) How does this deformation influence the local tilt and the shape of the NI interface? (3) What is the effect of the elastic forces on the line tension? Another interesting question concerns the structure of the liquid crystal in the core region, however, we do not consider this problem here.

To answer these questions we assume the Landau-de Gennes model in the form presented in section II. Note that anchoring at the NI interface depends on the sign of $L_2 + L_3$. If it is positive planar anchoring is stable, otherwise anchoring is homeotropic. These are the only stable configurations in the Landau-de Gennes theory [43]. Here, we follow the method of Kerins and Boiteux [44], who applied Noether's theorem [45] in their studies of an inhomegeneous multi-component fluid system, by means of the van der Waals theory, to derive the Neumann triangle conditions. We note, however, that Rey using an alternative approach in [46,47] has recently derived a generalized Young equation for the nematic-isotropic-substrate contact line. In [48], we present our approach based on Noether's theorem in more detail as well as the comparison with Rey's results.

According to Noether's theorem if the free energy density is invariant with respect to an arbitrary translation in the x-direction then one can construct a two-dimensional field of vanishing divergence, provided that the tensor **Q** satisfies the Euler-Lagrange equations. Since we consider a homogeneous substrate we can apply Noether's theorem to obtain the force balance equation. The field in question can be expressed in terms of a stress tensor defined as follows

$$\sum_{kl}^{e} = f\delta_{kl} - \frac{\partial f}{\partial(\partial_k Q_{ij})}\partial_l Q_{ij} \tag{3.2}$$

where δ_{kl} is the Kronecker δ. Σ^e is a natural generalization of the Ericksen stress tensor [1], defined originally in terms of the director field, to the interfacial regions, where also order parameters change. Now, for **Q** satisfying the Euler-Lagrange equations, the condition of hydrostatic equilibrium in the x direction follows:

$$\partial_x \sum_{xx}^{e} + \partial_z \sum_{zx}^{e} = 0 \tag{3.3}$$

To derive the Young condition we proceed as follows. (3.3) is integrated over a large but finite two-dimensional domain $\mathcal{A}$ containing the contact line, and then it is transformed into a contour integral over the boundary $\partial\mathcal{A}$. In principle, $\partial\mathcal{A}$ can be an arbitrary contour. However, in order to obtain meaningful physical quantities from the integral we assume the contour presented in Fig. 4. In the limit of infinite domain

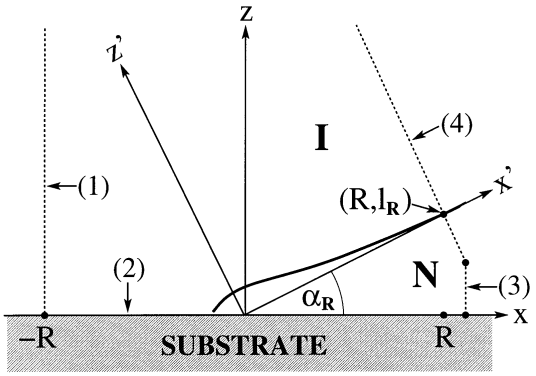

Figure 4. A fragment of the domain $\mathcal{A}$ considered in the text. The boundaries of $\mathcal{A}$ are shown as paths (1)–(4). The remaining boundary closing the contour $\partial\mathcal{A}$ in the bulk isotropic phase is not shown. The point (R, l_R) is on the NI interface, and α_R denotes the local tilt angle. The axis z' is normal to the NI interface at $x = R$.

the Young condition follows. An analogous procedure was applied by Kerins and Boiteux [44] to a simple fluid system to derive the Neumann triangle conditions. In the case of liquid crystals, it is reasonable to consider a domain whose boundaries are at some large but finite distance R from the contact line, where the interfacial and bulk regions are well defined. Since the deformation of $\hat{\mathbf{n}}$ in the bulk nematic phase decays very slowly with R we expect that this should have some effect on the balance of forces. Indeed, an asymptotic analysis for large R leads to the following force balance equation

$$\gamma_{NS} - \gamma_{IS} + \gamma_{NI}\cos\alpha_R + \sin\alpha_R \frac{\partial \gamma_{NI}}{\partial \theta'_{NI}} + \psi_{el} = 0 \tag{3.4}$$

where α_R denotes the local tilt angle of the NI interface. The last two terms are specific to liquid crystals and have no counterpart in simple fluid systems. They vanish, however, when $R \to \infty$. Then, the Young condition for $\alpha_c = \lim_{R\to\infty} \alpha_R$ is recovered. However, for large R, they give contributions of order R^{-1}. The first of them is due to the anchoring energy at the NI interface, where θ'_{NI} defines the director orientation with respect to the interface normal. Its presence in (3.4) means that apart from the usual tension acting parallel to the interface there is also a force of interfacial origin acting along the interface normal. Since the NI interface is tilted this force has a non-vanishing x component. The last term, denoted as ψ_{el}, represents the contribution to the contour integral due to the deformation of the director field in the bulk nematic phase.

From (3.1) and (3.4) we obtain the leading contributions to the local tilt of the NI interface as a function of the distance from the contact line:

$$\alpha_R \sim \alpha_c + \frac{K\cos\alpha_c}{2\gamma_{NI}R}\left[\left(\frac{\Delta\theta_a}{\alpha_c}\right)^2 - 1\right] \tag{3.5}$$

where K is the average of the splay and the bend elastic constants, and $\Delta\theta_a = \theta'_{NI} - \theta_{NS}$ is the difference in anchoring directions at the NI and the NS interfaces, measured with respect to their normals. (3.5) clearly shows that the shift of the tilt angle with respect to α_c depends on the type of anchoring at each interface. In the case of homeotropic anchoring ($\theta'_{NI} = \theta_{NS} = 0$), $\alpha_R < \alpha_c$, whereas in the case of mixed anchoring ($\theta'_{NI} = \pi/2$, $\theta_{NS} = 0$ or *vice versa*), $\alpha_R > \alpha_c$. The position of the NI interface over the substrate, l_R, can be obtained from (3.5) *via* the relation $dl_R/dR = \tan\alpha_R$, hence,

$$l_R \sim R\tan\alpha_c + \frac{K\ln(R/R_0)}{2\gamma_{NI}\cos\alpha_c}\left[\left(\frac{\Delta\theta_a}{\alpha_c}\right)^2 - 1\right] + l_0 \tag{3.6}$$

where R_0 is a cut-off length, and l_0 is the integration constant. Note that for large R, l_R deviates logarithmically from linear asymptotic behaviour expected for simple fluids. It is of interest to estimate the characteristic length scale $K/2\gamma_{NI}$, which appears in (3.5) and (3.6). Using the data for 5CB [49]: $K = 2.1\times10^{-7}$ erg cm^{-1} and $\gamma_{NI} = 1.5\times10^{-2}$ erg cm^{-2}, we find $K/2\gamma_{NI} = 700$ Å.

Finally, there remain the question about the line tension, τ, which is the excess free energy due to the presence of the contact line. The prescription for calculating τ is as follows [37,39]. Consider the excess free energy (over the bulk value) per unit length of the contact line of a two-dimensional domain of linear size R, containing the contact line. For large R, the dominant contribution comes from the interfacial tensions and it is proportional to R. The next order contribution is due to the line tension, and there are also lower order contributions, which decay when $R \to \infty$. Thus, in general, τ is a function of R, which may tend or not to a finite value when $R \to \infty$, *i.e.* in the thermodynamic limit. In simple fluid systems, this problem has been studied in the context of the transition from partial to complete wetting (see for instance [38] and references therein). A singular behaviour of τ at the wetting transition may occur if the effective interaction between the fluid-fluid interface and the substrate is of sufficiently long range. Here, although we do not study the wetting transition, we encounter a similar problem.

To study the behaviour of τ in the thermodynamic limit, we have developed a macroscopic approach analogous to the so-called interface displacement model [41,20], introduced in the context of simple fluid systems. In the framework of that model, one postulates or derives an effective interface Hamiltonian, which is a functional of $l(x)$, the distance of the fluid-fluid interface from the substrate. A formal derivation of the interface Hamiltonian has been proposed by several authors (see [50]). The case studied in this paper is different as the interface Hamiltonian should also contain orientational variables [51,52], *i.e.* the orientations of the director at the NS

($z = 0$) and the NI ($z = l(x)$) interfaces, denoted by $\theta_0(x)$ and $\theta_l(x)$, respectively. Thus, the excess free energy due to the contact line now becomes a functional of l, θ_0 and θ_l [48]. Its minimum corresponds to the equilibrium line tension. Using this macroscopic approach we can rederive (3.5), which means that it is consistent with the Landau-de Gennes theory. Moreover, it is straightforward to calculate the contribution to τ due to the elastic deformation of the director field. The main conclusion, concerning the behaviour of τ for large R, is as follows: In the case of homeotropic anchoring at both the NI and the NS interfaces, τ tends to a finite limit when $R \to \infty$. This is because an increase of the bulk free energy caused by the distortion of $\hat{\mathbf{n}}$ is cancelled out by a decrease of area of the NI interface, compared with linear $l(x)$, due to the logarithmic term (see (3.6)). No such a cancellation occurs, however, in the case of mixed anchoring at the interfaces. Then, the interfacial area increases compared with linear $l(x)$, and for large R, τ behaves like ln R, which means that it diverges in the thermodynamic limit.

IV. SMECTIC-A SURFACE ORDERING

Smectic surface order can appear at the free surface of the isotropic phase (coexisting with the vapour) or at the interface between the isotropic phase and a solid substrate, for some systems exhibiting a direct isotropic–smectic-A transition [53–56]. In these cases, the onset of the smectic order is compatible with the geometry of the system, *i.e*. the smectic layers are parallel to the limiting surfaces. There exists, however, another possibility when the interface favours parallel alignment of molecules. Then the smectic layers, if they were to form, should be oriented perpendicular to the interface. To be more specific, we consider the nematic phase in contact with a solid substrate and assume that it can undergo a direct first order transition to the smectic-A phase. Moreover, we assume that anchoring on the substrate is planar and monostable. In other words, the substrate is anisotropic and a particular direction of alignment in its surface is favoured, which is also referred to as homogeneous boundary conditions. An interesting possibility arises when the nematic order at the surface is enhanced compared to its bulk value. Although the presence of the substrate does not help directly the formation of smectic layers it may do so indirectly, due to the coupling between the nematic and smectic order parameters [1]. A similar situation occurs when a bulk nematic phase is placed in an external electric field. It was shown experimentally that the electric field can induce the nematic–smectic-A transition [57].

To study this problem, we apply again the Landau-de Gennes formalism. Now, the bulk free energy density, f_L, depends on both $\mathbf{Q}$ and the smectic order parameter, ψ, and is given by [58]

$$f_L = A\psi^2 + B\psi^4 + CTr\mathbf{Q}^2 + DTr\mathbf{Q}^3 + E(Tr\mathbf{Q}^2)^2 + \psi^2[FTr\mathbf{Q}^2 + G(\hat{\mathbf{k}}\cdot\mathbf{Q}\cdot\hat{\mathbf{k}}) + H(\hat{\mathbf{k}}\cdot\mathbf{Q}\cdot\hat{\mathbf{k}})^2 + L(\mathbf{Q}\cdot\hat{\mathbf{k}})^2] \quad (4.1)$$

where $\hat{\mathbf{k}}$ is normal to the smectic layers. f_L contains all invariants up to the fourth order. Since both the nematic and smectic-A phases are uniaxial, in the bulk $\mathbf{Q}$ has only one independent component. Thus, we can assume that $Q_{xx} = \eta$, $Q_{yy} = Q_{zz} = -\eta/2$, where the x axis is along the preferred direction in the plane of the substrate (the xy plane). After rescaling of the order parameters (4.1) reduces to

$$f_L = (t+1)\eta^2 - 2\eta^3 + \eta^4 + (a_0 + a_1\eta + a_2\eta^2)\psi^2 + \psi^4 \tag{4.2}$$

where t measures the temperature. To ensure that the smectic order does not exist without the nematic order, a_0 must be positive. When the temperature is lowered η increases, which should promote smectic ordering, therefore, we choose a negative a_1. Finally, $a_2 > -2$ is required by the stability condition for f_L. The system undergoes the NI transition at $t = t_{NI} = 0$, whereas the nematic–smectic-A transition occurs at $t = t_{NA} < 0$.

Close to the surface the liquid crystal is biaxial, which means that $Q_{yy} \neq Q_{zz}$. Here, however, we neglect this biaxiality and assume that the free energy depends only on two order parameters: η and ψ, hence, the contribution to the free energy density due to inhomogeneities is given by

$$f_G = \frac{1}{2}L_1\left(\frac{d\eta}{dz}\right)^2 + \frac{1}{2}L_2\left(\frac{d\psi}{dz}\right)^2 \tag{4.3}$$

Note that the elastic constants L_1 and L_2 should not be confused with the elastic constants that appear in (2.1c). Finally, the surface free energy is of the form given by (2.3), with only one non-vanishing component $h_{xx} = h$, hence, $f_s = -h\eta(z=0)$. Adding the bulk and the surface contributions we define the excess free energy as a functional of η and ψ, which is then minimized. The resulting Euler-Lagrange equations are solved numerically. The details of calculations are presented in [59].

To study surface transitions, it is convenient to introduce surface order parameters, which are the adsorptions: $\Gamma_\eta = \int_0^\infty [\eta(z) - \eta_N]dz$ and $\Gamma_\psi = \int_0^\infty \psi(z)dz$, where η_N is the bulk nematic order parameter, and we have assumed $t > t_{NA}$. A surface symmetry-breaking transition corresponds to the change of Γ_ψ from zero above the transition temperature, t_s, to $\Gamma_\psi \neq 0$ below t_s. Another surface transition that occurs in the system is the prewetting or the thin film-thick film transition, at which both Γ_η and Γ_ψ change discontinuously.

Possible topologies of the phase diagram in the (t,h) plane, obtained for different values of the ratio L_2/L_1, are shown in Figs. 5 and 6. We have fixed the values of the parameters in such a way that $t_{NA} = -2$. The dashed line represents a continuous symmetry-breaking surface transition, at which the onset of smectic-A ordering with layers perpendicular to the substrate appears. The solid line represents a first-order prewetting transition. It ends at a surface critical point (t_p^{cr}, h_p^{cr}), at which the difference between the thin and the thick films disappears. We observe three possible topolo-

gies: (1) the dashed line terminates at the line of the bulk nematic–smectic-A transition (Fig. 5a), (2) the dashed line terminates at the prewetting line (Fig. 5b), and (3) the dashed line is a continuation of the prewetting line, and the surface critical point becomes a tricritical point (Figs. 6a and 6b).

Let us consider first the topology shown in Fig. 5a. When the temperature is lowered from t_{NI} to t_{NA} at constant surface field we observe five possible behaviours of the system.

(i) For small h the system has always the nematic symmetry down to t_{NA}.

(ii) The system undergoes a continuous symmetry-breaking surface transition at $t = t_s(h)$ but the thickness of the smectic-A film remains finite when t approaches t_{NA}^{+} (partial wetting).

(iii) Apart from the symmetry-breaking transition there is a prewetting transition at $t = t_p(h) < t_s(h)$, at which both Γ_η and Γ_ψ jump to higher values. Both adsorptions diverge when $t \to t_{NA}^{+}$ (complete wetting by the smectic-A phase).

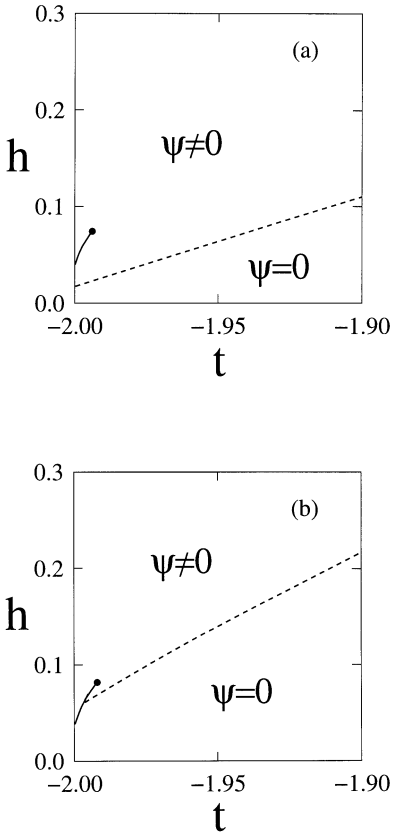

Figure 5. Surface phase diagram in the (t,h) plane for (a) $L_2/L_1 = 0$ and (b) $L_2/L_1 = 0.01$. The dashed line corresponds to the continuous surface transition discussed in the text, and the solid line to the prewetting transition.

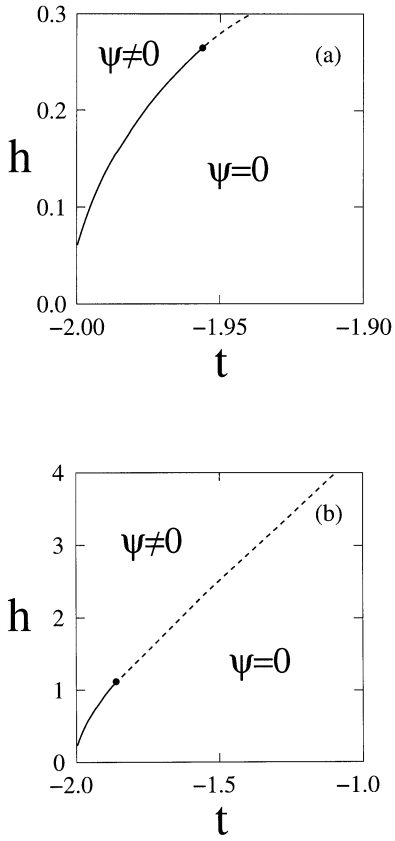

Figure 6. Surface phase diagram in the (t,h) plane for (a) $L_2/L_1 = 0.1$ and (b) $L_2/L_1 = 1$. The meaning of the lines is the same as in Fig. 5. Note the presence of a tricritical point instead of the surface critical point and the critical end point.

(iv) If $h > h_p^{cr}$ then there is only a continuous transition at $t = t_s(h)$, and $\Gamma_\eta, \Gamma_\psi \to \infty$ when $t \to t_{NA}^+$.

(v) For rather high values of h, the smectic-A surface order exists in the whole range $t_{NA} < t < t_{NI}$.

For the topology shown in Fig. 5b, there are also five possible behaviours of the system, depending on h. In this case, however, the line of the continuous surface transition terminates at a crtical end point, which lies on the prewetting line. Thus, the lower part of the prewetting line corresponds to the thin film-thick film transition with a symmetry change (Γ_ψ jumps from zero to a nonzero value), whereas the upper part corresponds to an ordinary prewetting transition without symmetry change.

The last possible topology of the phase diagram is shown in Figs. 6a and 6b, which differ from each other only quantitatively. In this case, the symmetry-breaking transition is either continuous or first order, and the first order transition is identical with the thin film-thick film transition.

V. CONCLUSIONS AND DISCUSSION

We have discussed three kinds of interrelated surface phenomena in liquid crystal systems: anchoring, wetting and surface symmetry breaking. From the wealth of anchoring phenomena we have chosen the case of an anisotropic substrate. In principle, possible types of anchoring can be obtained from a formal expansion in spherical harmonics of the effective surface free energy treated as a function of the bulk director [2,60]. It contains, however, unknown phenomenological parameters, the number of which increases with the order of the expansion. We have shown that using the Landau-de Gennes model we can reproduce all observed experimentally behaviours even with the simplest possible form of the bare surface free energy, containing only linear coupling with the surface order parameter. However, we expect to obtain a better quantitative agreement with experiment if also quadratic terms in the surface order parameter are included in f_s. A work along this line is currently in progress.

Anisotropy of the substrate turns out to be important for the observation of the symmetry-breaking transition discussed in section IV. Our mean field analysis, based on the Landau-de Gennes model, has shown that the onset of the smectic-A phase may appear in the surface layer before the bulk N–Sm-A transition. However, it is well known that in dimension $d = 3$ the smectic order is destroyed by thermal fluctuations. The average square of the layer fluctuation amplitude, $\langle u^2(\mathbf{r})\rangle$, diverges in the thermodynamic limit, albeit very slowly, like ln L, where L is the size of the system. This is known as the Landau-Peierls instability [1]. In consequence of this instability, the smectic order-parameter correlation function exhibits an algebraic decay, which means a quasi-long-range translational order [61]. In our surface problem, as long as the smectic film is not macroscopically thick, it should be treated as a quasi-two-dimensional system. Then the long wavelength contribution to $\langle u^2(\mathbf{r})\rangle$ is dominated by the modes with wavevectors in the plane of the substrate. In the absence of an ordering field $\langle u^2(\mathbf{r})\rangle$ would diverge like L (in $d = 2$), and the surface smectic order predicted by mean field would be destroyed by the fluctuation effect. However, in the presence of a surface ordering field, which breaks the isotropy of the substrate, we expect a quasi-long-range smectic order close to the substrate, as for a three-dimensional bulk smectic phase. This suggests that the surface symmetry-breaking transition might be a Kosterlitz-Thouless defect-unbinding transition [62,29], where the defects are edge dislocations [1]. In [59], we calculate the energy of an edge dislocation per unit length, or the line tension, in the presence of an external field that fixes the orientation of smectic layers far from the dislocation. We find that the line tension does not have a thermodynamic limit but diverges like ln L. This asymptotic behaviour supports the defect-unbinding scenario of the transition. We note finally that in view of a recent progress in computer simulations of hard rods at a hard wall it should be possible to simulate the nematic phase close to the bulk nematic–smectic-A transition. It would be interesting to check whether a microscopic model can confirm predictions of the Landau-de Gennes theory.

We have also applied the Landau-de Gennes theory to study partial wetting of the substrate by the nematic phase at the NI coexistence. The influence of anchoring on the shape of the NI interface and on the line tension, associated with the nematic-isotropic-substrate contact line, have been investigated. It was shown that in the case of mixed anchoring the line tension diverges in the thermodynamic limit. Our derivation of the force balance equation implicitly assumes that the distance of the NI interface from the substrate is much larger than the maximum of the extrapolation lengths of the NI and the NS interfaces, b_{max}. Then the director field in the bulk nematic phase is distorted. However, when anchoring is weak b_{max} is large, and close to the contact line l becomes comparable or smaller than b_{max}. This means that the distortion energy of the bulk director field becomes comparable to the energetic cost of unfavourable alignment of $\hat{\mathbf{n}}$ at the interface with weak anchoring. It is known that competition between different anchoring favoured by the NI and the NS interfaces may lead to a transition between two nematic phases, one of which is uniform and the other has a distorted director field. This may occur when the NI coexistence is approached from the isotropic phase, and a nematic wetting layer grows [28]. Only if is the wetting layer sufficiently thick the director field becomes distorted. Although we consider partial wetting, we also expect qualitatively different behaviours of the director field in the asymptotic regions: $l >> b_{max}$ and $l << b_{max}$. Therefore, it would be interesting to study the vicinity of the contact line in more detail, which we defer to future work.

Acknowledgment

The author's fee was financed by the Association for Author Rights Collective Administration of Scientific and Technical Works KOPIPOL with a seat in Kielce from the remuneration collected on the basis of Art. 20 of the Law on Author Right and Related Rights.

REFERENCES

1. de Gennes P.G. and Prost J., The Physics of Liquid Crystals, Oxford: Clarendon Press 1993.
2. Jérôme B., *Rep. Prog. Phys*., **54**, 391 (1991).
3. Yokoyama H., *Mol. Cryst. Liq. Cryst*., **165**, 265 (1988).
4. Janning J., *Appl. Phys. Lett*., **21**, 173 (1972).
5. Jérôme B., Pieranski P. and Boix M., *Europhys. Lett*., **5**, 693 (1988).
6. Monkade M., Boix M. and Durand G., *Europhys. Lett*., **5**, 697 (1988).
7. Jérôme B. and Pieranski P., *J. Phys. France*, **49**, 1601 (1988).
8. Barberi R. and Durand G., *Appl. Phys. Lett*., **58**, 2907 (1991).
9. Barberi R., Giocondo M. and Durand G., *Appl. Phys. Lett*., **60**, 1085 (1992).
10. Jägemalm P., Barbero G., Komitov L. and Zvezdin A.K., *Phys. Rev. E*, **58**, 5982 (1998).
11. Faetti S., Gatti M., Palleschi V. and Sluckin T.J., *Phys. Rev. Lett*., **55**, 1681 (1985).
12. Bechhoefer J., Duvail J-L., Masson L., Jérôme B., Hornreich R.M. and Pieranski P., *Phys. Rev. Lett*., **64**, 1911 (1990).
13. Jérôme B., O'Brien J., Ouchi Y., Stanners C. and Shen Y.R., *Phys. Rev. Lett*., **71**, 758 (1993).
14. Jérôme B. and Shen Y.R., *Phys. Rev. E*, **48**, 4556 (1993).
15. Jérôme B., *Mol. Cryst. Liq. Cryst*., **251**, 219 (1994).

16. Teixeira P.I.C. and Sluckin T.J., *J. Chem. Phys*., **97**, 1498 (1992); Teixeira P.I.C. and Sluckin T.J., *ibid*., **97**, 1510 (1992).
17. Zhu Y.M., Lu Z.H., Jia X.B., Wei Q.H., Xiao D., Wei Y., Wu Z.H., Hu Z.L. and Xie M.G., *Phys. Rev. Lett*., **72**, 2573 (1994).
18. Qian T.Z. and Sheng P., *Phys. Rev. Lett*., **77**, 4564 (1996).
19. Qian T.Z. and Sheng P., *Phys. Rev. E*, **55**, 7111 (1997).
20. de Gennes P.G., *Rev. Mod. Phys*., **57**, 827 (1985).
21. Dietrich S., in Phase Transitions and Critical Phenomena, Eds. C. Domb and J. Lebowitz, NY: Academic Press 1988, vol. 12, p. 1.
22. Schick M., in Liquids at Interfaces, Les Houches Summer School Lectures, Session XLVIII, Eds. J. Charvolin, J.F. Joanny and J. Zinn-Justin, Amsterdam: North-Holland 1990, p. 415.
23. Sluckin T.J. and Poniewierski A., in Fluid Interfacial Phenomena, Ed. C.A. Croxton, Chichester: Wiley 1986, Chap. 5.
24. Valignat M.P., Villette S., Li J., Barberi R., Bartolino R., Dubois-Violette E. and Cazabat A.M., *Phys. Rev. Lett*., **77**, 1994 (1996).
25. Vandenbrouck F., Bardon S., Valignat M.P. and Cazabat A.M., *Phys. Rev. Lett*., **81**, 610 (1998).
26. Rodríguez-Ponce I., Romero-Enrique J.M., Velasco E., Mederos L. and Rull L.F., *Phys. Rev. Lett*., **82**, 2697 (1999).
27. Alkhairalla B., Allinson H., Boden N., Evans S.D. and Henderson J.R., *Phys. Rev. E,* **59**, 3033 (1999).
28. Braun F.N., Sluckin T.J. and Velasco E., *J. Phys.: Condens. Matter*, **8**, 2741 (1996).
29. Sluckin T.J. and Poniewierski A., *Phys. Rev. Lett*., **55**, 2907 (1985).
30. Kothekar N., Allender D.W. and Hornreich R.M., *Phys. Rev. E*, **49**, 2150 (1994).
31. L'vov Y., Hornreich R.M. and Allender D.W., *Phys. Rev. E*, **48**, 1115 (1993).
32. Poniewierski A., *Phys. Rev. E*, **47**, 3396 (1993).
33. van Roij R., Dijkstra M. and Evans R., *Europhys. Lett*., **49**, 350 (2000).
34. Sen A.K. and Sullivan D.E., *Phys. Rev. A*, **35**, 1391 (1987).
35. Teixeira P.I.C., Sluckin T.J. and Sullivan D.E., *Liq. Cryst*., **14**, 1243 (1993).
36. Poniewierski A. and Samborski A., *Liq. Cryst*., **27**, 1285 (2000).
37. Rowlinson J.S. and Widom B., Molecular Theory of Capillarity, Oxford: Clarendon Press 1982.
38. Indekeu J.O., *Int. J. Mod. Phys. B*, **8**, 309 (1994).
39. Widom B. and Widom H., *Physica A*, **173**, 72 (1991).
40. Szleifer I. and Widom B., *Mol. Phys*., **75**, 925 (1992).
41. Indekeu J.O., *Physica A*, **183**, 439 (1992).
42. Perković S., Blokhuis E.M. and Han G., *J. Chem. Phys*., **102**, 400 (1995).
43. de Gennes P.G., *Mol. Cryst. Liq. Cryst*., **12**, 193 (1971).
44. Kerins J. and Boiteux M., *Physica A*, **117**, 575 (1983).
45. Lovelock D. and Rund H., Tensors, Differential Forms and Variational Principles, NY: Wiley 1975.
46. Rey A.D., *Liq. Cryst*., **27**, 195 (2000).
47. Rey A.D., *J. Chem. Phys*., **111**, 7675 (1999).
48. Poniewierski A., *Liq. Cryst*., **27**, 1369 (2000).
49. Faetti S. and Palleschi V., *Phys. Rev. A*, **30**, 3241 (1984).
50. Rejmer K. and Napiórkowski M., *Phys. Rev. E*, **53**, 881 (1996).
51. Sullivan D.E. and Lipowsky R., *Can. J. Chem*., **66**, 553 (1988).
52. Sluckin T.J. and Poniewierski A., *Mol. Cryst. Liq. Cryst*., **179**, 349 (1990).
53. Ocko B.M, Braslau A., Pershan P.S., Als-Nielsen J. and Deutsch M., *Phys.Rev.Lett*., **57**, 94 (1986).
54. Somoza A.M., Mederos L. and Sullivan D.E., *Phys. Rev. Lett*., **72**, 3674 (1994).
55. Selinger J.V. and Nelson D.R., *Phys. Rev. A*, **37**, 1736 (1988).
56. Pawlowska Z., Sluckin T.J. and Kventsel G.F., *Phys. Rev. A*, **38**, 5342 (1988).
57. Lelidis I. and Durand G., *Phys. Rev. Lett*., **73**, 672 (1994).
58. Poniewierski A. and Sluckin T.J., *Mol. Phys*., **73**, 199 (1991).
59. Poniewierski A. and Samborski A., *Phys. Rev. E*, **51**, 4574 (1995).
60. Fournier J.-B. and Galatola P., *Phys. Rev. Lett*., **82**, 4859 (1999).
61. Caillé A., *C.R. Acad. Sci*., **274B**, 891 (1972).
62. Kosterlitz M. and Thouless D.J., *J. Phys. C*, **6**, 1181 (1973).